Nuclear Inst. and Methods in Physics Research, A 924 (2019) 297–300

Contents lists available at ScienceDirect

Nuclear Inst. and Methods in Physics Research, A

journal homepage: www.elsevier.com/locate/nima

Diamond detector technology, status and perspectives

H. Kagan [13,*], A. Alexopoulos [3], M. Artuso [20], F. Bachmair [24], L. Bäni [24], M. Bartosik [3], J. Beacham [13], H. Beck [23], V. Bellini [2], V. Belyaev [12], B. Bentele [19], P. Bergonzo [11], A. Bes [27], J.-M. Brom [7], M. Bruzzi [4], G. Chiodini [26], D. Chren [18], V. Cindro [9], G. Claus [7], J. Collot [27], J. Cumalat [19], A. Dabrowski [3], R. D'Alessandro [4], D. Dauvergne [27], W. de Boer [10], S. Dick [13], C. Dorfer [24], M. Dunser [3], V. Eremin [6], G. Forcolin [22], J. Forneris [15], L. Gallin-Martel [27], M.-L. Gallin-Martel [27], K.K. Gan [13], M. Gastal [3], C. Giroletti [17], M. Goffe [7], J. Goldstein [17], A. Golubev [8], A. Gorišek [9], E. Grigoriev [8], J. Grosse-Knetter [23], A. Grummer [21], B. Gui [13], M. Guthoff [3], I. Haughton [22], B. Hiti [9], D. Hits [24], M. Hoeferkamp [21], T. Hofmann [3], J. Hosslet [7], J.-Y. Hostachy [27], F. Hügging [1], C. Hutton [17], J. Janssen [1], K. Kanxheri [28], G. Kasieczka [24], R. Kass [13], F. Kassel [10], M. Kis [5], G. Kramberger [9], S. Kuleshov [8], A. Lacoste [27], S. Lagomarsino [4], A. Lo Giudice [15], E. Lukosi [25], C. Maazouzi [7], I. Mandic [9], C. Mathieu [7], M. Menichelli [28], M. Mikuž [9], A. Morozzi [28], J. Moss [29], R. Mountain [20], S. Murphy [22], M. Muškinja [9], A. Oh [22], P. Olivero [15], D. Passeri [28], H. Pernegger [3], R. Perrino [26], F. Picollo [15], M. Pomorski [11], R. Potenza [2], A. Quadt [23], A. Re [15], M. Reichmann [24], G. Riley [25], S. Roe [3], D. Sanz [24], M. Scaringella [4], D. Schaefer [3], C.J. Schmidt [5], D.S. Smith [13], S. Schnetzer [14], S. Sciortino [4], A. Scorzoni [28], S. Seidel [21], L. Servoli [28], B. Sopko [18], V. Sopko [18], S. Spagnolo [26], S. Spanier [25], K. Stenson [19], R. Stone [14], C. Sutera [2], A. Taylor [21], B. Tannenwald [13], M. Traeger [5], D. Tromson [11], W. Trischuk [16], C. Tuve [2], J. Velthuis [17], N. Venturi [3], E. Vittone [15], S. Wagner [19], R. Wallny [24], J.C. Wang [20], J. Weingarten [23], C. Weiss [3], T. Wengler [3], N. Wermes [1], M. Yamouni [27], M. Zavrtanik [9]

[1] *Universität Bonn, Bonn, Germany*
[2] *INFN/University of Catania, Catania, Italy*
[3] *CERN, Geneva, Switzerland*
[4] *INFN/University of Florence, Florence, Italy*
[5] *GSI, Darmstadt, Germany*
[6] *Ioffe Institute, St. Petersburg, Russia*
[7] *IPHC, Strasbourg, France*
[8] *ITEP, Moscow, Russia*
[9] *Jožef Stefan Institute, Ljubljana, Slovenia*
[10] *Universität Karlsruhe, Karlsruhe, Germany*
[11] *CEA-LIST Technologies Avancees, Saclay, France*
[12] *MEPHI Institute, Moscow, Russia*
[13] *The Ohio State University, Columbus, OH, USA*
[14] *Rutgers University, Piscataway, NJ, USA*
[15] *University of Torino, Torino, Italy*
[16] *University of Toronto, Toronto, ON, Canada*
[17] *University of Bristol, Bristol, UK*
[18] *Czech Technical University, Prague, Czech Republic*
[19] *University of Colorado, Boulder, CO, USA*
[20] *Syracuse University, Syracuse, NY, USA*
[21] *University of New Mexico, Albuquerque, NM, USA*
[22] *University of Manchester, Manchester, UK*
[23] *Universität Goettingen, Goettingen, Germany*

* Corresponding author.
E-mail address: harris.kagan@cern.ch (H. Kagan).

https://doi.org/10.1016/j.nima.2018.06.009
Received 6 March 2018; Received in revised form 6 May 2018; Accepted 4 June 2018
Available online 7 June 2018

[24] ETH Zürich, Zürich, Switzerland
[25] University of Tennessee, Knoxville, TN, USA
[26] INFN-Lecce, Lecce, Italy
[27] LPSC-Grenoble, Grenoble, France
[28] INFN-Perugia, Perugia, Italy
[29] California State University, Sacramento, CA, USA

ARTICLE INFO

Keywords:
Chemical vapor deposition
pCVD diamond
Diamond detectors
3D diamond detectors
Radiation tolerant detectors

ABSTRACT

Detectors based on Chemical Vapor Deposition (CVD) diamond have been used extensively and successfully in beam conditions/beam loss monitors as the innermost detectors in the highest radiation areas of Large Hadron Collider (LHC) experiments. The startup of the LHC in 2015 brought a new milestone where the first polycrystalline CVD (pCVD) diamond pixel modules were installed in an LHC experiment and successfully began operation. The RD42 collaboration at CERN is leading the effort to develop polycrystalline CVD diamond as a material for tracking detectors operating in extreme radiation environments. The status of the RD42 project with emphasis on recent beam test results is presented.

1. Introduction

The RD42 collaboration [1,2] at CERN is leading the effort to develop radiation tolerant devices based on pCVD diamond as a material for tracking detectors operating in harsh radiation environments. Diamond has properties which make it suitable for such detector applications. During the last few years the RD42 group has succeeded in producing and measuring a number of devices to address specific issues related to use at the HL-LHC [3,4]. This paper presents the status of the RD42 project with emphasis on recent beam test results. In particular, results are presented on the status of the first diamond pixel detector based on pCVD material, on the independence of signal size on incident particle rate in pCVD diamond detectors over a range of particle fluxes up to 20 MHz/cm^2 and on the 3D diamond detectors fabricated in pCVD diamond.

2. Status of the ATLAS diamond beam monitor

The startup of the LHC in 2015 brought a new milestone for diamond detector development where the first planar diamond pixel modules based on pCVD diamond were installed in an LHC experiment, the ATLAS experiment [5], and successfully began operation. The ATLAS Diamond Beam Monitor (DBM) [6,7] was designed to measure the instantaneous luminosity, the background rates and the beam spot position. A single DBM module consists of an 18 mm × 21 mm pCVD diamond 500 μm thick instrumented with a FE-I4 pixel chip [8]. The 26,880 pixels are arranged in 80 columns on 250 μm pitch and 336 rows on 50 μm pitch resulting in an active area of 16.8 mm × 20.0 mm. This fine granularity provides high precision particle tracking. The deposited charge from a particle is measured in the FE-I4 by Time-over-Threshold.

The ATLAS DBM uses diamonds with a charge collection distance (the average distance an electron–hole pair move apart under the influence of the applied electric field) of 200–220 μm at an applied bias voltage of 500 V. Three telescopes each with 3 diamond DBM modules (plus 1 telescope with silicon sensors) mounted as a three layer tracking device were installed inside the pixel detector services on each side of the ATLAS interaction point at 90 cm $< |z| <$ 111 cm, $3.2 < |\eta| < 3.5$ and at a radial distance from 5 cm to 7 cm from the center of the beam pipe. The modules have an inclination of 10°with respect to the ATLAS solenoid magnetic field direction to suppress erratic dark currents [9] in the diamonds. The ATLAS DBM data-acquisition system is shared with the ATLAS IBL [10]. After initial installment, data were collected in the July 2015 run. These data have been analyzed and the first results of the ATLAS DBM tracking capabilities are shown in Fig. 1. A clear separation between background particles from unpaired bunches (open circles) and collision particles from colliding bunches (filled circles) is observed. After two electrical incidents in 2015 with consequent loss of several silicon and diamond modules, the DBM has now been re-commissioned and is again in the operation phase.

3. Rate studies in pCVD diamond

In order to study the dependence of signal size on incident particle rate, RD42 performed a series of beam tests in the πM1 beam line of the High Intensity Proton Accelerator (HIPA) at Paul Scherrer Institute (PSI) [11]. This beam line is able to deliver 260 MeV/c π^+ fluxes from a rate of ∼5 kHz/cm^2 to a rate ∼20 MHz/cm^2 in bunches spaced 19.8 ns apart.

Sensors using pCVD material [12] were tested in a tracking telescope [13] based on 100 μm × 150 μm silicon pixel sensors read out by the PSI46v2 pixel chip [14]. The diamond signals were amplified with custom-built front-end electronics with a peaking time of ∼6 ns, return-to-baseline in ∼16 ns and 550e noise with 2 pf input capacitance. The amplified signals were recorded with a DRS4 evaluation board [15] operating at 2 GS/s. The entire system was triggered with a scintillator which determined the timing of the beam particles with a precision of ∼0.7 ns.

A series of cuts were applied to the data including: removing 60 s of triggers at the beginning of each run, removing triggers from heavily ionizing particles with saturated waveforms (mostly protons), removing calibration triggers, removing triggers in the wrong beam bucket, removing triggers with no tracks in the telescope and removing triggers with large angle tracks in the telescope. After applying this procedure all telescope tracks which project into the diamond fiducial region have a pulse height well separated from the pedestal distribution in the diamond i.e. the diamond is 100% efficient at all rates. The same procedure was applied to all particle flux points and the resulting mean pulse height (in arbitrary units) versus rate is shown in Fig. 2 for both positive and negative bias voltage. The uncertainty on the data points in the plot include both statistical and systematic sources. The systematic uncertainty was determined by assuming any deviations in pulse height for rates below 80 kHz/cm^2 were due to systematic effects. Thus the spread in the data points at a given rate indicates the reproducibility of the data. Fig. 2 indicates the mean pulse height in pCVD diamond detectors irradiated up to 5×10^{14} n/cm^2 does not depend strongly on rate up to rates of 20 MHz/cm^2.

4. 3D diamond pixel detectors

3D sensors with electrodes in the bulk of the sensor material were first proposed in 1997 [16] in order to reduce the drift distance of the

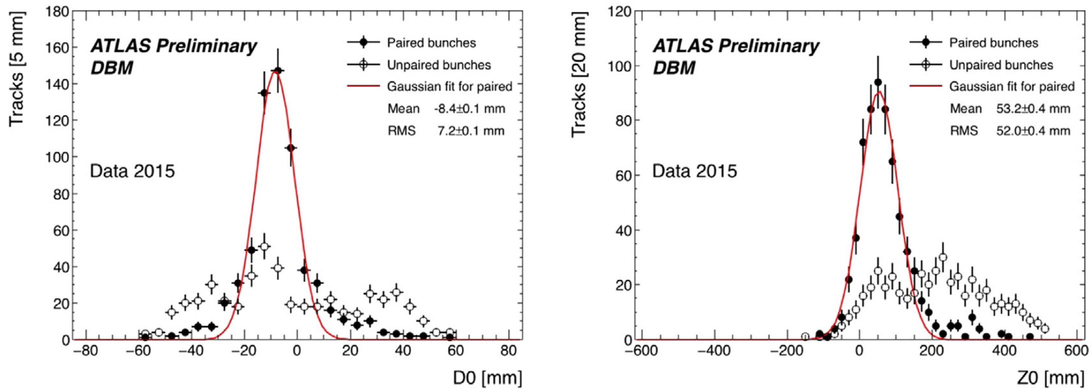

Fig. 1. Radial distance (left plot) and longitudinal distance (right plot) of the closest approach of the projected particle tracks to the interaction point as recorded by a single DBM telescope with preliminary alignment.

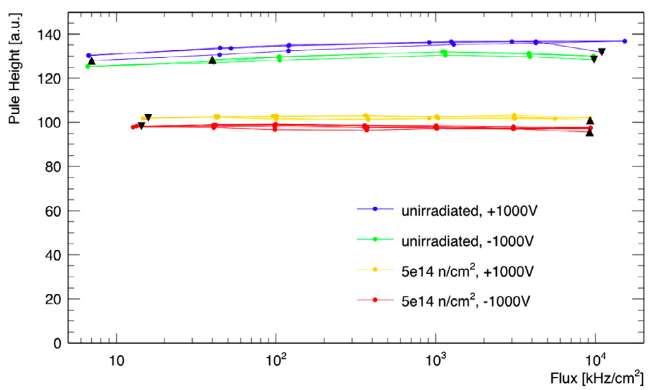

Fig. 2. The average pulse height versus rate for an un-irradiated and irradiated pCVD diamond pad detector at positive and negative bias. The beam line parameters were adjusted to set the different particle rates. The data was taken by scanning up and down in rate multiple times. The pulse height units are arbitrary since the un-irradiated and irradiated detectors used different readout electronics. The resulting electronics gain corrections and the relative gain correction for positive versus negative signals in the electronics is still being determined and has not been applied.

charged carriers to much less than the sensor thickness. In order to achieve this goal a series of alternating + and − electrodes perpendicular to the read out face were created in the bulk detector material. This idea is particularly beneficial in detectors with a limited mean free path such as trap dominated sensor materials like heavily irradiated silicon and pCVD diamond where the observed signal size is related to the mean free path divided by the drift distance. Under these circumstances one gains radiation tolerance (larger signals) by keeping the drift distance less than the mean free path. With this geometrical structure charge carriers drift inside the bulk parallel to the surface over a typical drift distance of 25–100 μm instead of perpendicular to the surface over a distance of 250–500 μm.

In 2015 RD42 published results of a 3D device fabricated in single-crystal CVD diamond [17] showing that the 3D structure works in diamond. In 2016 RD42 fabricated the first 3D device in pCVD diamond [18]. The electrodes in the bulk of the pCVD diamond 3D device were fabricated with lasers as described in [17]. The bias electrodes were placed at the corners and the readout electrodes were placed in the middle of the cells. This pCVD device was shown to collect more than 75% of the deposited charge which translates in more than a factor of two more charge than a planar diamond strip detector fabricated on the same pCVD diamond.

In 2017 RD42 successfully constructed the first pCVD diamond 3D pixel detector with 50 μm × 50 μm cells. This pixel device is designed to be read out with the RD53 pixel readout chip [19] which is not yet available. In order to read this device out with an existing pixel readout chip a small number of cells were ganged together to match the pitch of the pixel readout chip. RD42 is proceeding to make 3D diamond pixel devices compatible with both the CMS pixel readout chip (3×2 ganging) and the ATLAS pixel readout chip (1×5 ganging). The first 50 μm × 50 μm pCVD diamond 3D pixel device which was bump-bonded used the CMS pixel readout chip.

This first diamond 3D pixel device was tested during the Aug 2017 beam test at PSI at a single voltage and with rates from 7 kHz/cm^2 to 7 MHz/cm^2. During the initial lab test it was discovered that the bump bonding had a small issue on one edge. We decided to take data with the device rather than try to repair this small bump bonding issue. Fig. 3 (left) shows the preliminary efficiency as a function of xy position for every cell in the device with a 1500e pixel threshold. The red box marks the fiducial region used to measure the hit efficiency. The blue circle indicates the position of the one non-working pixel cell in the central region of the device. Fig. 3 (right) shows the hit efficiency in the fiducial region with the 1500e pixel threshold as a function of time during an up–down scan of incident particle rates from 7 kHz/cm^2 to 7 MHz/cm^2 and back to 7 kHz/cm^2. The overall measured efficiency is 99.2% and no change in efficiency as a function of rate is observed. The corresponding efficiency for a planar silicon CMS pixel detector in this test was 99.7% with no change in efficiency as a function of rate. The slight loss of efficiency (0.5%), assuming it holds through the completion of the analysis, is most likely due to charge loss in the column electrodes. If this explanation is correct, then this effect can be easily remedied by tilting the detector at a small angle with respect to the incident beam.

5. Conclusions

The recent progress in the design, fabrication and testing of polycrystalline CVD diamond detectors was presented. The following milestones have been achieved: successful operation of the first pCVD diamond planar pixel detector in the ATLAS experiment at the LHC; demonstration that the average signal pulse height of pCVD diamond detectors irradiated up to 5×10^{14} n/cm^2 is independent of the particle flux up to ~20 MHz/cm^2; successful fabrication and operation of the first pCVD diamond 3D pixel detector with 50 μm × 50 μm pixels read out with CMS pixel electronics where the efficiency for a MIP was >99% and the average charge collected in the device was >90% of the deposited charge. In the future RD42 plans to study the pulse height dependence of CVD diamond sensors with pad and pixel electrodes with radiation doses up to 10^{17} n/cm^2 and continue the development of 3D diamond detectors with the production of a 50 μm × 50 μm cell pCVD diamond 3D pixel detector compatible with ATLAS readout electronics.

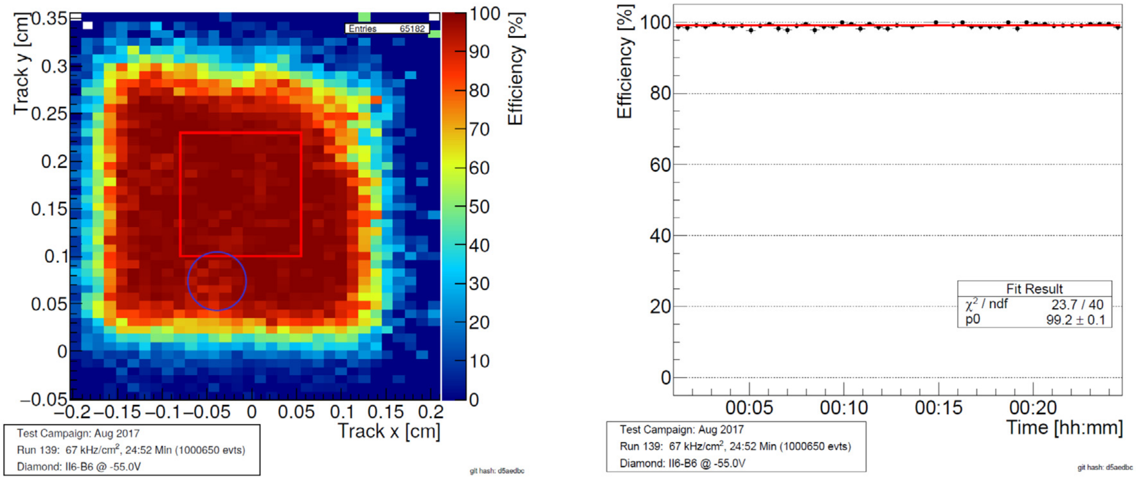

Fig. 3. The hit efficiency of the first 50 μm × 50 μm cell pCVD 3D pixel detector with 3 × 2 ganged cells read out with CMS pixel electronics with a 1500e threshold. The left plot shows the efficiency of each ganged cell as a function of xy position in the device. The right plot shows the average efficiency in the fiducial region (the red box in the left plot) as a function of time during the run at 67 kHz/cm^2. (For interpretation of the references to color in this figure legend, the reader is referred to the web version of this article.)

Acknowledgments

The RD42 Collaboration gratefully acknowledges the staff at CERN for test beam time and their help in setting up the beam conditions. We would especially like to thank Henric Wilkens, the test beam coordinator, for his assistance in making our tests a success. We also thank the beam line staff at the PSI High Intensity Proton Accelerator especially Konrad Deiters, Manuel Schwarz and Davide Reggiani for their assistance in carrying out the diamond detector tests. We extend our gratitude to Prof. Lin Li and David Whitehead of the University of Manchester Laser Processing Center for their assistance in the production of 3D diamond devices. The research leading to these results received funding from the European Union's Horizon 2020 research and innovation program under grant agreement No. 654168. This work was also partially supported by the Swiss National Science Foundation grant # 20FL20_154216, ETH grant 51 15-1, Royal Society Grant UF120106 and the U.S. Department of Energy through grant DE-SC0010061.

References

[1] W. Adam, et al. [RD42 collaboration], Development of Diamond Tracking Detectors for High Luminosity Experiments at the LHC, Proposal/RD42 CERN/DRDC 94-21, Status Report/RD42, CERN/LHCC, 95-43, 95-53, 95-58, 97-03, 98-20, 2000-011, 2000-015, 2001-002, 2002-010, 2003-063, 2005-003, 2006-010, 2007-002, 2008-005.

[2] M. Artuso, et al. [RD42 Collaboration], RD42 Status Report: Development of Diamond Tracking Detectors for High Luminosity Experiments at the LHC, CERN-LHCC-2017-006.

[3] G. Apollinari, et al., Chapter 1: High-Luminosity Large Hadron Collider HL-LHC in High-Luminosity Large Hadron Collider (HL-LHC): Preliminary Design Report, CERN Yellow Reports: Monographs, CERN-2015-005, CERN Geneva, 2015. http://dx.doi.org/10.5170/CERN-2015-005.1.

[4] G. Apollinari, et al., High-Luminosity Large Hadron Collider (HL-LHC): Technical Design Report V01, CERN Yellow Reports: Monographs, Volume 4/2017 CERN-2017-007-M, CERN Geneva 2017. http://dx.doi.org/10.23731/CYRM-2017-004.

[5] G. Aad, et al. [ATLAS collaboration], The ATLAS experiment at the CERN Large Hadron Collider, JINST 3 (2008) S08003.

[6] H. Kagan, et al., ATLAS Diamond Beam Monitor TDR, ATLAS Document DBM, 001, 2011.

[7] M. Červ, et al., The ATLAS diamond beam monitor, JINST 9 (2014) C02026.

[8] M. Barbero, et al., The FE-I4 pixel readout chip and the IBL module, PoS(Vertex 2011) 038, 2011.

[9] A.J. Edwards, et al., Radiation monitoring with diamond sensors in BABAR, IEEE Trans. Nucl. Sci. 51 (2004) 1808.

[10] F. Huegging, et al. [ATLAS Collaboration], The ATLAS pixel insertable b-layer (IBL), Nucl. Instrum. Methods Phys. Res. A 650 (2011) 45.

[11] PSI High Intensity Proton Accelerator, High Energy Beam Lines. http://www.psi.ch/abe/high-energy-beam-lines.

[12] The diamond material for these tests was provided by II-VI Inc., 360 Saxonburg Road, Saxonburg, PA.

[13] F. Bachmair, CVD Diamond Sensors In Detectors For High Energy Physic (Ph.D thesis), ETH Zürich, 2016. http://dx.doi.org/10.3929/ethz-a-010748643.

[14] H.Chr. Kästli, et al., Design and performance of the CMS pixel detector readout chip, Nucl. Instrum. Methods Phys. Res. A 565 (2006) 188.

[15] S. Ritt, DRS4 Evaluation Board, http://www.psi.ch/drs/evaluation-board.

[16] S. Parker, C.J. Kenney, J. Segal, 3-D: A proposed new architecture for solid state radiation detectors, Nucl. Instrum. Methods Phys. Res. A 395 (1997) 328.

[17] F. Bachmair, et al. [RD42 Collaboration], A 3D Diamond detector for particle tracking, Nucl. Instrum. Methods Phys. Res. A 786 (2015) 97.

[18] A. Alexopoulos, et al. [RD42 Collaboration], Diamond detector technology: status and perspectives, PoS(Vertex 2016) 027, 2016.

[19] M. Garcia-Sciveres, et al. [RD53 Collaboration], The RD53A Integrated Circuit, CERN-RD53-PUB-17-001, 2017. https://cds.cern.ch/record/2287593?ln=en.